Development of Thermal Model by Performance Verification of Heat Pipe Subsystem for Electronic Cooling under Space Environment

MK Lee, JS Hong, SM Sin, and HU Oh

Abstract—Heat pipes are used to control the thermal problem for electronic cooling. It is especially difficult to dissipate heat to a heat sink in an environment in space compared to earth. For solving this problem, in this study, the Poiseuille (Po) number, which is the main measure of the performance of a heat pipe, is studied by CFD; then, the heat pipe performance is verified with experimental results. A heat pipe is then fabricated for a spatial environment, and an in-house code is developed. Further, a heat pipe subsystem, which consists of a heat pipe, MLI (Multi Layer Insulator), SSM (Second Surface Mirror), and radiator, is tested and correlated with the TMM (Thermal Mathematical Model) through a commercial code. The correlation results satisfy the 3K requirement, and the generated thermal model is verified for application to a spatial environment.

Keywords—CFD, Heat pipe, Radiator, Space.

I. INTRODUCTION

THE thermal management problem becomes more severe due to increasing heat concentration for electronic components as they become smaller while their performance is enhanced. A spatial environment with only radiation for heat dissipation is more severe compared to earth. For this reason, a variety of heat pipe studies have been performed regarding both space and earth.

Oh et al. [1] studied the design and fabrication of a metallic micro heat pie using the laser-induced wet etching technique. Aghanajafi et al. [2] conducted numerical simulation of fully developed flow for characteristic laminar slip flow and heat transfer in rhombus micro-channels with radiation to examine the effect of the Po number under various aspect ratios. Park et al. [3] proposed a method for the design for micro-fluidic systems by considering the Po number and using CFD. Using a lumped-layer model, Jin et al. [4] conducted performance analysis of a heat pipe radiator for the thermal control of satellites.

MK Lee is with the Mechatronics Group, Samsung Thales Co. Ltd., Yongin-City, Republic of Korea (Corresponding author's details – Phone: +82-31-8020-7318; Fax: +82-31-8020-7350; e-mail: mk2.lee@samsung.com).

JS Hong is with the Mechatronics Group, Samsung Thales Co. Ltd., Yongin-City, Republic of Korea (e-mail: js.hong@samsung.com).

SM Sin is with the Image Information Systems Development Division, Agency for Defense Development, Daejoen-city, Republic of Korea (e-mail: ssm@add.re.kr).

HU Oh is with the Image Information Systems Development Division, Agency for Defense Development, Daejoen-city, Republic of Korea (e-mail:ohu314@add.re.kr).

In this study, a thermal model for heat pipe subsystems under a high-vacuum environment that simulates a spatial environment is developed and verified by a thermal balance test and the TMM (Thermal Mathematical Model) correlation; using CFD, the heat pipe performance is examined in relation to the Po number.

II. THE POISEUILLE NUMBER

The heat pipe performance depends on the working fluid, channel geometry, and pipe material. As the operating condition is already determined, the variable parameter for heat pipe design is only the channel geometry. Therefore, the Po number should be investigated. To calculate the Po number, the momentum equation of the incompressible flow reduces as follows:

$$\frac{\partial^2 u}{\partial y^2} + \frac{\partial^2 u}{\partial z^2} = \frac{1}{\mu}\frac{dp}{dx} = \text{constant}. \qquad (1)$$

In (1), u is the local velocity, p is the local pressure, μ is the viscosity, x is the axial coordinate, and y and z are the lateral coordinates. In this flow, the Poiseuille number is defined as:

$$Po = -\frac{1}{\mu}\frac{dp}{dx}\frac{D^2}{2V}. \qquad (2)$$

In (2), D is the hydraulic diameter and V is the mean velocity. For one-dimensional flow with a constant channel shape, the number is constant. (1) is the classic Poisson equation and used as indicated in [5]. FLUENT software was used. The study has focused on only rectangular channels of convectional heat pipes. The computational domain was discretized with structural homogenous meshes. The mesh size was sufficient to achieve results that were independent of the mesh structure. The obtained results are presented in TABLE I and Fig. 1. TABLE I shows the computational results regarding the Po number in comparison to [3]; the two sets of results are similar. Fig. 1 illustrates the internal velocity distribution of rectangular channels; the distribution is seen to be of a general type in comparison with [3].

TABLE I
COMPUTED RESULTS FOR THE PO NUMBER AND A COMPARISON

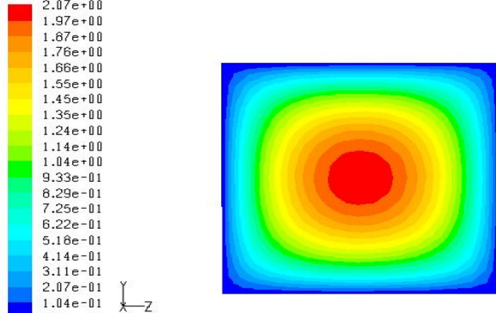| Aspect ratio	Present result	[6]
1.0	14.18	14.22

POISEUILLE NUMBER FOR RECTANGULAR CHANNEL FLOW

Fig. 1. Contour plot describing the flow profile in a rectangular channel.

As can be observed in Fig. 1, FLUENT is able to represent the Po number and by comparison with [6], the calculated parameter can be verified for use for numerous channel geometries.

III. VERIFICATION OF THE HEAT PIPE MODEL

Heat pipe performance analysis has been conducted with many simulation methods [7]. But, this research is performed in view of design limitations for heat pipe operation. There are several design limitations for heat pipes such as capillary, sonic, entrainment, and boiling limitations. One of the most critical limitations is known as the capillary limitation, and the equation for capillary limitation is represented by the heat-transport factor $(QL)_{c,max}$ [8]:

$$(QL)_{c,max} = \int_0^{L_t} Q dx$$

$$= \frac{\dfrac{2\sigma}{r_c} - \Delta P_\perp - \rho_l g L_t \sin\varphi}{F_l + F_v}$$

Where, $\hspace{3cm}$. $\hspace{2cm}$ (3)

$$F_l = \frac{\mu_l}{K A_\omega \rho_l \lambda}$$

$$F_v = \frac{(f_v \operatorname{Re}_v) \mu_v}{2 r_{h,v}^2 A_v \rho_v \lambda}$$

The main design parameter depends on F_v, which is a function of the Po number. In this study, the results are applied to the heat pipe characteristic equation, which is developed with an in-house code.

For verifying the developed in-house code, heat pipe performance analysis was performed using advanced experimental results [9]. TABLE II shows the experimental

TABLE II
HEAT PIPE GEOMETRY FOR ANALYSIS [9]

Item	Specification
Inner diameter	10.27mm
Outer diameter	14.71mm
Number of grooves	25
Working fluid	NH₃, 99.9999%
Pipe material	Al, 6063-T6
Total length	1422.4mm
Evaporator length	127mm
Condenser length	127mm

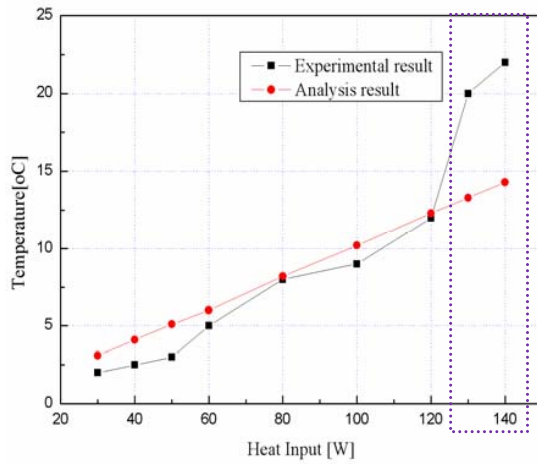heat pipe geometry used in [9] for model verification.

Fig. 2. Comparison of the experimental and analytic results according to the heat input.

Based on the experimental data in TABLE II, following [8], heat pipe analysis was performed for each heat input in terms of the temperature difference for the entire length.

$$Q = A_p (T_{p,e} - T_{p,c})[\frac{\pi r_o^2 \ln(r_o / r_i)}{2\pi L_e k_p} +$$

$$\frac{\pi r_o^2 \ln(r_i / r_v)}{2\pi L_e k_{e,e}} + \frac{\pi r_o^2 T_v (P_{v,e} - P_{v,c})}{\rho_v \lambda J Q}$$

$$+ \frac{\pi r_o^2 \ln(r_i / r_v)}{2\pi L_c k_{e,c}} + \frac{\pi r_o^2 \ln(r_0 / r_i)}{2\pi L_c k_p}]^{-1}$$

(4)

In (4), the unknown values are ΔP_v at the evaporator, adiabatic section, and condenser. Each average pressure difference is represented as follows [8].

$$Average\ \Delta P_v\ at\ evaporator = \frac{F_v \int_0^{L_e} \int_0^x Q t dt dx}{L_e} = \frac{F_v L_e Q}{6} .$$

$$\Delta P_v\ at\ adiabatic\ section = F_v L_a Q .$$

$$Average\ \Delta P_v\ at\ condenser = \frac{F_v L_c Q}{6}\ .$$

By achieving the pressure differences, the temperature differences within heat pipes are calculated using (4).

Fig. 2 presents the analytic and experimental results were similar to each other. However, the results for heat inputs of 130W and 140W were different from the current analytic results. Heat pipe burn-out is predicted to have occurred at the section due to a large heat input. Through these results, the developed in-house code for heat pipe performance was verified using the calculated Po number.

IV. THERMAL BALANCE TEST FOR THE HEAT PIPE SUBSYSTEM

A heat pipe should be designed for maintaining the electronic performance within the operating range in a spatial environment. Heat pipes for space are mainly exposed to a high-vacuum environment without convection. Therefore, this heat dissipation unit depends on radiation that is oriented to the temperature of deep space, viz., 3K. For this study, the electronic unit was a compressor but the thermal dummy was substituted by a cartridge heater. Fig. 3 shows the thermal dummy for a compressor that is equipped with a cartridge heater of about 35W.
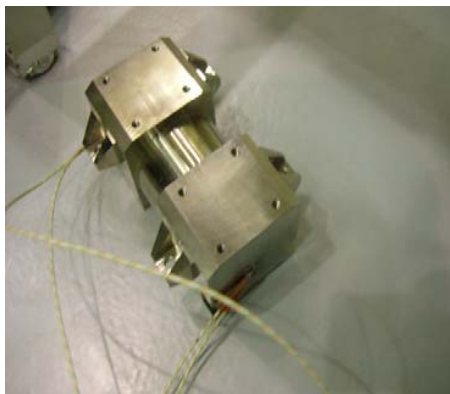

Fig. 3. Thermal dummy with a cartridge heater for the compressor.

The heat pipe subsystem consisted of a heat pipe, radiator, MLI (Multi Layer Insulator), and SSM (Second Surface Mirror), as shown in Fig. 4. The test-room environmental conditions were as follows.

- Temperature: 22℃±3℃.

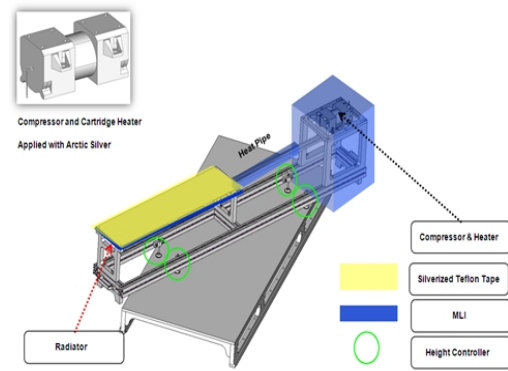- Relative humidity: 55%±5%.

- Ambient pressure: 500~1050hPa.

Fig. 4. Concept diagram of a heat pipe subsystem.

The thermal balance test was performed using a high-vacuum chamber under a shroud wall temperature of -150℃ and pressure of 1X 10^{-5} Torr; the chamber was 1.5m in diameter and 1m in length. In terms of solar-flux simulation, a solar-flux heater was used for the back side of the radiator.

Fig. 5. Heat pipe subsystem in a vacuum chamber.

Fig. 5 illustrates the heat pipe subsystem in the vacuum chamber. A radiator with an SSM (yellow dotted line) was exposed to the shroud wall in keeping with -150℃ for heat exchange through radiation. But, the SSM was substituted by silverized Teflon tape owing to problems associated with delivery and cost during the thermal balance test. Even though silverized Teflon tape was applied, the test results could be obtained with the given optical properties of silverized Teflon tape. Aside from that, every component was covered with an MLI for protection from heat exchange from the shroud wall. The MLI was designed to isolate heat transfer from the chamber wall to the subsystem. It was also useful to reduce the large fluctuations in the temperature that were caused by changes in the temperature of the chamber wall. The effective emissivity was calculated using the following [10].

$$\varepsilon_{eff} = (0.000136\frac{1}{4\sigma T_m^2} + 0.000121 T_m^{0.667}) f_N f_A f_p\ . \tag{5}$$

In (5), σ is the Stefan-Boltzmann constant, Tm is the average temperature of MLI, f_N is a function of the number of layers, f_P

is a function of the penetration, and f_A is a function of the area. f_A is described by the following [10]:

$$f_A = \frac{1}{10^{(0.372\log A)}}, \qquad (6)$$

where A is the surface area of MLI. The observed test temperatures were used.

Before the thermal balance test, the TMM (Thermal Mathematical Model) was investigated using SINDA software for designing the radiator area on a hot case, which is the worst case for operating a stable heat pipe subsystem, solar-flux heater, and temperature-compensation heater. For the subsystem under consideration, steady-state thermal analysis based on the numerical, implicit Forward-Backward method, was used. The heat balance for a diffusive node is given as [11].

$$\frac{2C_i}{\Delta t}(T_i^{n+1} - T_i^n) = 2Q_i +$$
$$\sum_{j=1}^{N}\left[G_{ji}(T_j^n - T_i^n) + G_{ji}\left\{(T_j^n)^{\hat{4}} - (T_i^n)^4\right\}\right] + \qquad . \qquad (7)$$
$$\sum_{j=1}^{N}\left[G_{ji}(T_j^{n+1} - T_i^{n+1}) + G_{ji}\left\{(T_j^n)^{\hat{4}} - (T_i^{n+1})^4\right\}\right]$$

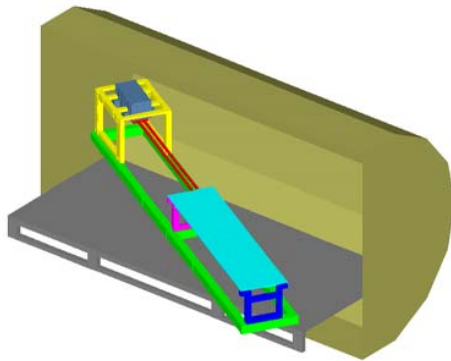Fig. 6 shows the TMM geometry for the heat pipe subsystem mesh geometry under SINDA software.

Fig. 6. TMM mesh geometry.

These analytic results had to comply with the experimental results to 3℃ for the given system requirements. Fig. 7 represents the temperature distribution on the heat pipe subsystem. The temperature difference between the compressor and the radiator was about 2℃. This is because heat transfer was well accomplished by the heat pipe with a very small gap temperature.
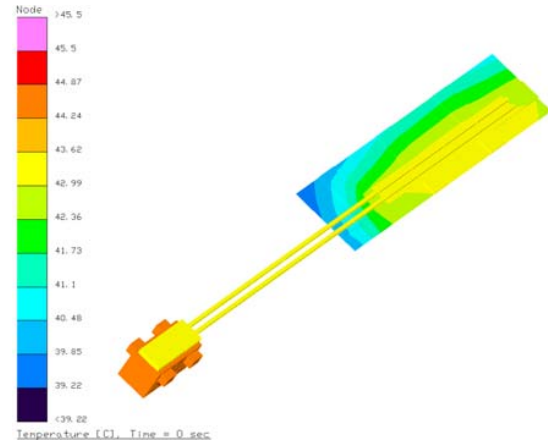

Fig. 7. Temperature distribution on the heat pipe subsystem.

The TMM correlation was developed by extracting the measured data from the thermal balance test. The purpose of the correlation was to control design parameters, such as the thermal contact resistance.
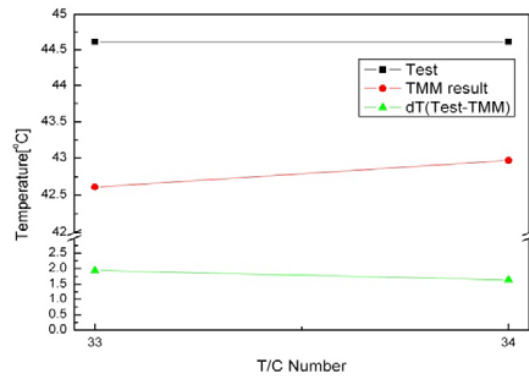

Fig. 8. Results of the TMM correlation regarding the compressor for the heat pipe subsystem.
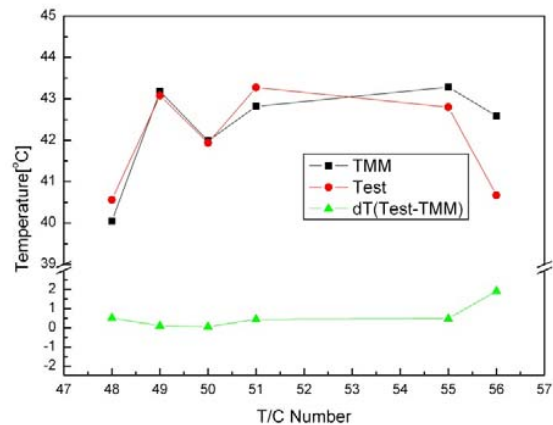

Fig. 9. Results of the TMM correlation regarding the radiator for the heat pipe subsystem.

Figs. 8 and 9 show the TMM correlation results. The

temperature difference was similar to the experimental result and the temperature requirement was also satisfied for every T/C (thermocouple) index. Fig. 10 illustrates the positions of the thermocouples for the TMM correlations. The thermocouples on the solar-flux heater were excluded because the sensors were more sensitive about heater temperature. The developed thermal model for the heat pipe subsystem was verified using the thermal balance test.
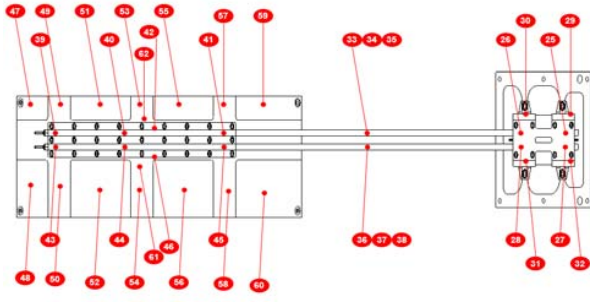

Fig. 10. Positions of the thermocouples.

V. CONCLUSION

A thermal model was developed by the performance verification of a heat pipe subsystem in a spatial environment. It was found that the rectangular channel characteristic could be calculated by obtaining the Po number using CFD. The heat-pipe performance was verified by comparison with experimental results. The TMM model well met with the requirements in light of the results of the thermal balance test. Thus, we expect to be able to develop electronic components for heat dissipation units in a spatial environment in the near future.

NOMENCLATURE

A_p	Cross-sectional area based upon the external pipe diameter [m^2]
A_w	Cross-sectional area of the wick [m^2]
C_i	Heat capacitance of diffusion thermal node i
G_p	Linear conductor for connecting the diffusion thermal nodes.
G_{ji}	Radiative conductor for connecting diffusion thermal node j to thermal node i.
J	Mechanical equivalent of heat
k_e	Effective thermal conductivity of the liquid-saturated wick [W/m-k]
$k_{e,c}$	Effective thermal conductivity of the liquid-saturated wick at the condenser [W/m-k]
$k_{e,e}$	Effective thermal conductivity of the liquid-saturated wick at the evaporator [W/m-k]
k_p	Thermal conductivity of the pipe material [W/m-k]
K	Wick permeability
L_a	Length of the adiabatic section of the heat pipe [m]
L_c	Length of the condenser section of the heat pipe [m]
L_e	Length of the evaporator section of the heat pipe [m]
$P_{v,c}$	Vapor pressure at the condenser [N/m^2]
$P_{v,e}$	Vapor pressure at the evaporator [N/m^2]
$\Delta P_\perp$	Hydrostatic pressure in the direction perpendicular to the pipe axis [N/m^2]
Q_i	Heat source/heat sink for diffusion thermal node j
$r_{h,v}$	Hydraulic radius of the wick at the vapor-wick interface [m]

r_i	Internal radius of the pipe [m]
r_o	External radius of the pipe [m]
r_v	Vapor core radius [m]
$T_{p,c}$	Condenser pipe wall temperature [^{o}C]
$T_{p,e}$	Evaporator pipe wall temperature [^{o}C]
T_j	Temperature of thermal node j at the current time, t
T_{j+1}	Temperature of thermal node j at the current time, t+Δt

Greek symbols

λ	Latent heat of vaporization [J/kg]
μ_v	Vapor dynamic viscosity kg/m-s]
ρ_l	Liquid density [kg/m^3]

REFERENCES

[1] K. H. OH, M.K. LEE, and S.H.JEONG, "Design and fabrication of a metallic micro-heat pipe based on high-aspect-ratio microchannels," Heat transfer engineering, vol. 28, pp. 8–9, 2007.

[2] C. Aghanajafi, V. Vandadi, M.R. Shahnazari, " Investigation of Convection and Radiation Heat Transfer in Rhombus Microchannels," Int. J. Research and Reviews in Applied Sciences, vol 3. Issue 2, 2010

[3] S.J. Park, S. Cjung, H.W. Bang, C.I. Chung, D.C. Han, J.K. Chang, "Modeling and Designing of Microfludic System Using Poiseuille Number," 2nd Annual International IEEE-EMBS Special Topic Conference on Microtechnologies in Medicine and Bilology. Proceedings(Cat.No.02EX578), 2002

[4] S.H. Jin and J.H. Boo, "Performance Analysis of a Heat Pipe Radiator for Thermal Control of Satellites," unpublished, 1992

[5] N. Damean, P.P.L. Regtien, "Poiseuille number for the fully developed laminar flow through hexagonal ducts etched in <100> silicon," Sensors and Actuators A, vol. 90, pp. 96-101, 2001

[6] R.K. Shah, "Laminar flow friction and forced convection heat transfer in ducts of arbitrary geometry," Int. J. Heat Transfer, vol. 18, pp. 849-862, 1975

[7] A. Faghri and M. Buchko "Experimental and Numerical Analysis of Low-Temperature Heat Pipes with Multiple Heat Sources" Transactions of ASME: Journal of Heat Transfer, Vol. 113, pp. 728-734, 1991

[8] Chi, S.W., Heat Pipe Theory and Practice, New York, pp 54, 1976

[9] T.H. Kim, "An Experimental Study on Estimation of Heat Transport Capability for the Cross Section of Axially Grooved Heat Pipes", unpublished, 2001

[10] Gilmore, David G.,"Spacecraft Thermla Control Handbook", The Aerospace Press, El Segundo, CA., 2002

[11] "SINDA/FLUINT User's Manual, Version 5.2", 2009, Cullimore and Ring Technologies, Inc.

Minkyu Lee received master's degree from the Department of Mechatronics at the Gwangju Institute of Science and Technology(South Korea), in 2006.
He is currently an engineer in the R & D division at Samsung Thales. His research interests include micro heat pipe, loop heat pipe, and Infra-Red camera imaging system in the field of mechanical engineering